Journal of Power Sources 265 (2014) 132–139

Contents lists available at ScienceDirect

Journal of Power Sources

journal homepage: www.elsevier.com/locate/jpowsour

Effect of organic solvent addition to $PYR_{13}FSI$ + LiFSI electrolytes on aluminum oxidation and rate performance of $Li(Ni_{1/3}Mn_{1/3}Co_{1/3})O_2$ cathodes

Tyler Evans [a], Jarred Olson [b], Vinay Bhat [b], Se-Hee Lee [a,*]

[a] Department of Mechanical Engineering, University of Colorado, Boulder, CO 80309, USA
[b] Boulder Ionics Corporation, Arvada, CO 80007, USA

HIGHLIGHTS

- LiFSI is superior in suppressing Al oxidation in $PYR_{13}FSI$ electrolytes.
- Addition of EC:EMC to $PYR_{13}FSI$ ILs leads to higher $t_{+,\,Li}$ and σ_{ionic}.
- IL-organic solvent mixtures enable high rate performance of $Li(Ni_{1/3}Mn_{1/3}Co_{1/3})O_2$.

GRAPHICAL ABSTRACT

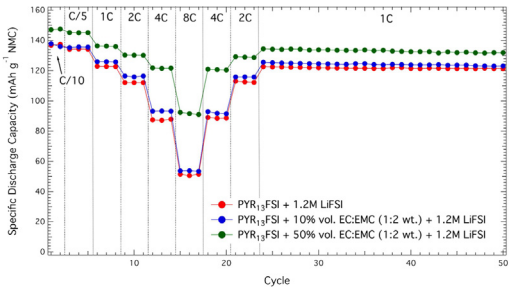

ARTICLE INFO

Article history:
Received 2 January 2014
Received in revised form
25 February 2014
Accepted 28 April 2014
Available online 6 May 2014

Keywords:
Ionic liquids
$PYR_{13}FSI$
LiFSI
Aluminum current collector
Corrosion

ABSTRACT

The superior suppression of aluminum current collector oxidation by a 1.2 M LiFSI in $PYR_{13}FSI$ ionic liquid electrolyte is demonstrated. Addition of EC:EMC (1:2 wt.) is shown to significantly increase the severity of parasitic aluminum oxidation. Despite leading to increased aluminum oxidation at high voltages (>4.2 V vs. Li/Li^+), adding organic solvent to $PYR_{13}FSI$ based ionic liquids greatly enhances important electrochemical properties. The ionic conductivity and lithium ion transference number of the $PYR_{13}FSI$ + 1.2 M LiFSI electrolyte increase with increasing volumetric content of organic co-solvent (EC:EMC), resulting in significant improvements to high rate performance. The electrochemical benefits of organic co-solvent addition and the compatibility of the $PYR_{13}FSI$ + 1.2 M LiFSI electrolyte with $Li(Ni_{1/3}Mn_{1/3}Co_{1/3})O_2$ demonstrated in this study substantiate the need to develop strategies to suppress aluminum oxidation during high voltage cycling of lithium-ion batteries in ionic liquid electrolytes.

1. Introduction

While lithium-ion batteries (LIBs) offer a potentially game-changing energy storage technology, safety concerns have hindered their widespread penetration into the electric vehicle market and have discouraged their consideration in grid level applications. Many of these safety concerns stem from the utilization of volatile organic electrolytes. Currently commercialized LIB technology is based on electrolytes comprised of mixtures of organic carbonate solvents containing lithium hexafluorophosphate ($LiPF_6$) as a salt. These electrolytes are preferred due to their high ionic conductivities and compatibility with commercialized electrode materials, but their flammability and high volatility must be addressed [1,2].

In order to mitigate electrolyte related safety risks without realizing a loss in performance, a new class of non-aqueous electrolyte should be developed. Due to their non-flammability,

* Corresponding author. Tel.: +1 303 492 7889; fax: +1 303 492 3498.
E-mail address: sehee.lee@colorado.edu (S.-H. Lee).

http://dx.doi.org/10.1016/j.jpowsour.2014.04.138
0378-7753/

negligible vapor pressures, thermal stabilities, high voltage stability windows, and sufficient ionic conductivities, room temperature ionic liquids (RTILs or ILs) represent promising options as additives or drop-in replacements for organic electrolytes in LIBs [3–8]. Extensive efforts are being made to develop high performance RTIL based electrolytes that are compatible with state of the art electrode materials [9–19], with a number of studies demonstrating the favorable electrochemical properties of pyrrolidinium-based ionic liquids [20,21] and ionic liquids containing the bis(trifluoromethanesulfonyl)imide ($TFSI^-$) [22–26] or bis(fluoro sulfonyl)imide (FSI^-) anion [8–10,20,22,27–35]. Recent research has shown that pyrrolidinium and imidazolium FSI-based ionic liquids have higher conductivities compared to their corresponding TFSI-based analogs due to lower solution viscosities [9,16,29,36] as well as adequate compatibility with electrode materials such as graphite, $LiCoO_2$, and $Li(Ni_{1/3}Mn_{1/3}Co_{1/3})O_2$ [9,11]. Despite these efforts to develop high performance electrolytes based on the FSI chemistry, improvements in ionic conductivity must be made in order to compete with commercialized organic electrolytes.

Various strategies can be employed to enhance the electrochemical performance of IL based electrolytes. By lowering the viscosity of ionic liquids using organic solvents, significant increases in ionic conductivity and lithium ion mobility can be achieved [4,13,37,38]. Addition of an organic solvent has also been shown to improve solid-electrolyte interphase (SEI) formation and stability on low voltage anode materials such as lithium metal or graphite [14,34,39–43]. Unfortunately, the addition of organic solvent to certain FSI and TFSI based ILs leads to a severe parasitic side reaction involving oxidation of the aluminum metal conventionally used as a current collector substrate on the cathode of LIBs [23,44,45]. While work has been done to characterize the solvent dependent oxidative dissolution mechanism for aluminum corrosion in TFSI-based electrolytes, relatively little work has been done to characterize similar effects in FSI-based electrolytes and the influence of such electrolyte solutions on electrochemical cycling performance.

This study examines the electrochemical properties of *N*-methyl-*N*-propyl-pyrrolidinium bis(fluorosulfonyl)imide ($PYR_{13}FSI$) ILs, developing a deeper understanding of the effect of increasing co-solvent content in $PYR_{13}FSI$-based electrolytes on aluminum oxidation behavior. Most notably, this research substantiates the electrochemical benefits of adding organic solvents to ILs by demonstrating increased ionic conductivities, increased Li^+ transference numbers, and the improved high rate performance of $Li(Ni_{1/3}Mn_{1/3}Co_{1/3})O_2$ in mixtures of $PYR_{13}FSI$ and carbonate solvent. Chronoamperometry, cyclic voltammetry (CV), and scanning electron microscopy (SEM) were used to identify parasitic aluminum corrosion via the oxidative dissolution mechanism, and potentiogalvanostatic cycling was utilized to characterize the effect of aluminum oxidative dissolution on battery cycling and rate performance of $Li(Ni_{1/3}Mn_{1/3}Co_{1/3})O_2$ half-cells with $PYR_{13}FSI$ + 1.2 M LiFSI based electrolytes.

2. Experimental

2.1. Electrolyte preparation

$PYR_{13}FSI$ was the ionic liquid selected for this study. Ionic liquid solutions were provided by Boulder Ionics Corporation (U.S.A.) and scanned for halide impurities. Impurities (F^-, Cl^-, Br^-, SO_4^-) were quantified using a Dionex ICS-1100 ion chromatograph, calibrated for sensitivities as low as 1 ppm. All ionic liquids and lithium salts used in this study were subjected to ion chromatography, and the total impurity content of every solution prepared was calculated based off the mass percentage of electrolyte component in the total mass of the electrolyte. The solutions contained less than 20 ppm (w/w) of moisture and less than 10 ppm (w/w) of halide and metal-ion impurities. Ethylene carbonate (EC):ethyl methyl carbonate (EMC) (BASF) mixed in a 1:2 weight ratio was utilized as organic co-solvent and added to the $PYR_{13}FSI$ electrolytes in 10% vol. and 50% vol. mixtures. LiFSI or LiTFSI, provided by Boulder Ionics Corp., was added in a 1.2 M concentration subsequent to mixing of the electrolyte solvents.

2.2. Electrode/electrochemical cell fabrication

To evaluate the aluminum corrosion behavior, high-grade aluminum foil (ESPI Metals; 25 μm thick; >99.5% purity) was punched into 1.27 cm diameter disks, rinsed in dimethyl carbonate (DMC) and dried at 120 °C in a vacuum oven for 12 h before testing. Composite electrodes were fabricated using $Li(Ni_{1/3}Mn_{1/3}Co_{1/3})O_2$ powder material (Johnson Controls), acetylene black (Alfa Aesar, AB) as a conductive additive, and polyvinyldene fluoride (Kynar, PVDF) binder in a weight ratio of (85:7.5:7.5). The composite was cast onto clean, high-grade aluminum foil current collector using a 5 mil doctor blade to achieve an active material mass loading of approximately 3 mg cm^{-2}. The electrodes were dried for 12 h at 80 °C. In order to ensure adequate electrical contact and to improve overall energy density, the electrodes were calendared to 75% of their initial thickness. Electrode disks of 1.27 cm diameter were punched and then dried at 120 °C in a vacuum oven for 12 h before testing.

Corrosion cells contained a high-grade aluminum foil disk working electrode and lithium foil counter electrode. Electrochemical cycling tests utilized $Li(Ni_{1/3}Mn_{1/3}Co_{1/3})O_2$ positive electrodes and lithium foil negative electrodes. Both configurations were assembled in aluminum clad 2032 coin-type cells (Pred/Hohsen). Glass microfibre filters (Whatman; grade GF/F) were wetted with the IL-EC:EMC solutions and used as the electrolyte separator.

2.3. Electrochemical characterization

Cyclic voltammetry was performed on corrosion cells by cycling potential between 3.0 V and 4.6 V vs. Li/Li^+ at a scan rate of 1 mV s^{-1} (Solartron 1280C). Chronoamperometry was performed on aluminum corrosion cells containing each electrolyte solution. Assembled corrosion cells containing each electrolyte composition were allowed to rest for 5 min. The working electrode potential was ramped from open circuit voltage (OCV) to 4.2 V vs. Li/Li^+ at a sweep rate of 1 mV s^{-1} and held for 12 h; the potential was then ramped from 4.2 V to 4.6 V vs. Li/Li^+ at a sweep rate of 1 mV s^{-1} and held for 24 h (Arbin BT2000). The current was continuously monitored during voltage ramps and holds. Subsequent to chronoamperometry, corrosion cells were disassembled and the aluminum foil working electrode was washed in DMC. Low-vacuum scanning electron microscopy (JEOL SEM 6480LV) was performed on the surface of the Al electrode.

Lithium transference number, $t_{+,\,Li}$, was determined for electrolytes containing LiFSI salt using the potentiostatic polarization (PP) method devised by Bruce and Vincent et al. [46,47] and adapted for liquid electrolytes, including IL based electrolytes [48–50]. EIS and potentiostatic polarization (Solartron 1280C) were performed on cells containing lithium foil electrodes, which were scraped clean to ensure minimal charge transfer resistance, in coin-type cells. EIS was performed between a frequency range of 20 kHz–10 mHz with an a.c. amplitude of 10 mV. σ_{ionic} was determined for electrolytes containing LiFSI using the standard complex impedance method on a Solartron 1280C for a frequency range of 20 kHz–10 mHz. Constant current–constant voltage (CC–

CV) cycling of $Li(Ni_{1/3}Mn_{1/3}Co_{1/3})O_2$ half-cells was carried out between 3.0 and 4.2 V vs. Li/Li^+ and 3.0–4.5 V vs. Li/Li^+ at room temperature in Al clad coin-type cells (Arbin BT2000). Rate studies were carried out with discharge/charge rates increasing to 8C before extended cycling at a rate of 1C, with the 1C rate corresponding to a current density of about 380 μA cm^{-2}.

3. Results and discussion

3.1. Oxidation behavior of aluminum current collector

Preliminarily, an experimental matrix was designed to systematically characterize the compatibility of $PYR_{13}FSI$ + 1.2 M LiFSI electrolytes with the aluminum current collector substrate during cycling of high voltage cathode materials. These results were compared with a similar study of 1.2 M LiTFSI in $PYR_{13}FSI$ in order to gain further insight into the electrochemical performance of $PYR_{13}FSI$ when coupled with different lithium salts. Previous work suggests that electrolyte solutions comprised of LiFSI salt in organic solvent are capable of suppressing aluminum oxidation more effectively than combinations of the same solvent with LiTFSI salt [9]. Our results prove that the same is true in $PYR_{13}FSI$-based electrolytes.

Inspection of the initial CV cycle of corrosion cells containing $TFSI^-$ based salt reveal irreversible anodic currents indicative of aluminum oxidation on the surface of the metal. This effect increases in magnitude with the addition of organic solvent. Fig. 1 presents initial CV cycles and chronoamperometric data for electrolytes containing $TFSI^-$. The most severe oxidative behavior occurs in the solution containing 50% vol. organic solvent (Fig. 1a), with the initial CV shape representing that of typical aluminum corrosion CV curves [45,46]. Chronoamperometric data supports this finding. During prolonged charging at 4.6 V vs. Li/Li^+, oxidative current densities exceeded 70 μA cm^{-2} in the solution containing 50% vol. organic solvent and remained under 5 μA cm^{-2} and 2 μA cm^{-2} in corrosion cells containing 10% vol. organic solvent and pure IL, respectively (Fig. 1b). As currents are observed to increase during chronoamperometry of cells containing organic solvent, it is determined that $TFSI^-$ is unable to successfully passivate the aluminum current collector surface. The solvent dependent current amplitudes shown in CV and chronoamperometry are in agreement with a previous study conducted by Kühnel et al. [23] on $PYR_{14}TFSI$-solution induced aluminum corrosion, but the significantly lower current amplitudes found in our work lead us to believe that the FSI^- anion in the ionic liquid is itself capable of suppressing aluminum oxidation to some degree.

Inspection of the initial CV cycle of aluminum foil discs in $PYR_{13}FSI$ + 1.2 M LiFSI solutions reveal much lower irreversible oxidative current densities than those seen with $PYR_{13}FSI$ + 1.2 M LiTFSI solutions. Fig. 2 presents initial CV cycles and chronoamperometric data for electrolytes containing FSI^-. Oxidative current densities observed during CV of corrosion cells with FSI-based ILs are also dependent on volumetric content of organic solvent, reaching 1.44 μA cm^{-2} in solutions containing 50% vol. organic solvent (Fig. 2a). Chronoamperograms of aluminum corrosion cells in the same solutions reveal significant aluminum oxidation only in cells containing organic solvent (Fig. 2b). During a 24 h constant voltage period at 4.6 V vs. Li/Li^+, oxidative currents reach about 8 μA cm^{-2} in cells containing 50% vol. organic solvent and remain below 4 μA cm^{-2} and 1 μA cm^{-2} for cells containing 10% vol. organic solvent and pure IL, respectively. As the oxidative current densities for cells containing pure ionic liquid and 10% vol. organic solvent do not continually increase over prolonged charging, it is determined that the FSI^- anion is able to passivate the aluminum surface to a higher degree than $TFSI^-$. This demonstrates

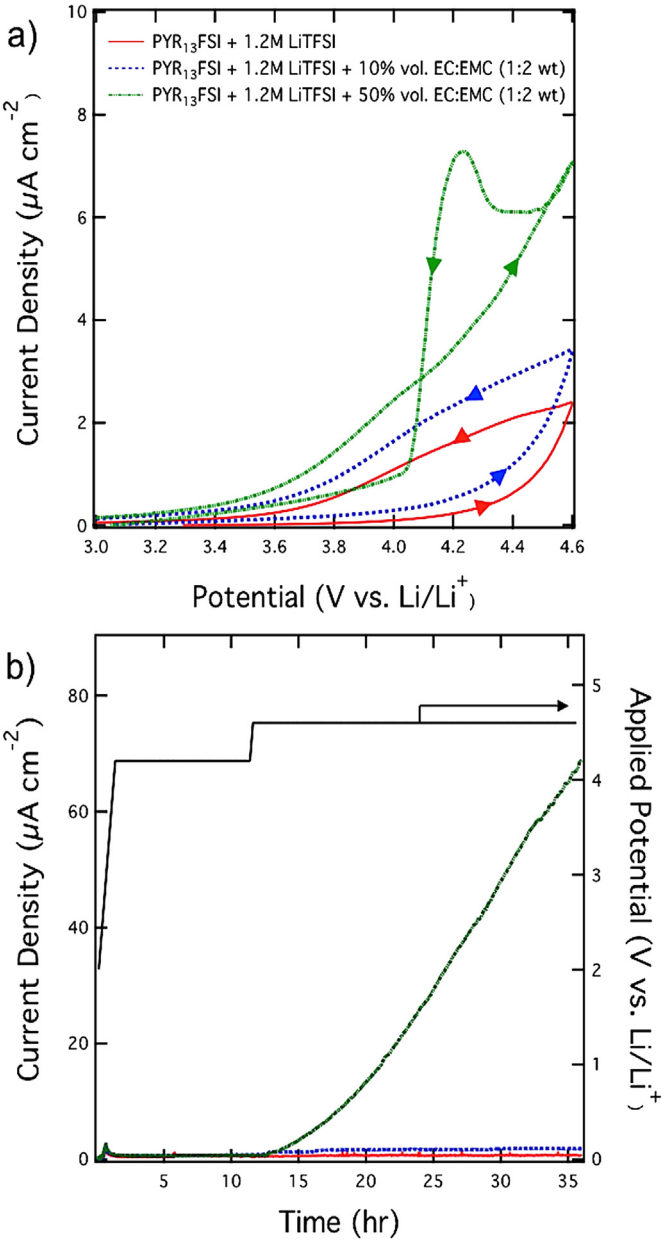

Fig. 1. Cyclic voltammograms (a) showing the first voltage scans and chronoamperograms (b) of aluminum corrosion cells with electrolyte solutions comprised of mixtures of $PYR_{13}FSI$ + 1.2 M LiTFSI and various volumetric amounts of EC:EMC (1:2 wt.).

that the LiFSI salt is strongly favored for protection against aluminum oxidation in $PYR_{13}FSI$ based electrolytes.

High-resolution SEM micrographs provided in Fig. 3 show that the oxidative current densities observed in CV and chronoamperometry resulted in significant changes to the Al foil's surface morphology. Fig. 3a–c indicates visible corrosion by solutions containing LiTFSI salt, with surface corrosion becoming most severe in the solution containing 50% vol. organic solvent. Large pits were formed on the Al sample charged in the solution containing 50% vol. organic solvent, with pit diameters approaching 300 μm. Non-uniform coloring in the SEM images is also indicative of corrosion, as gradients in shading represent changes in the sample's surface roughness. The Al samples charged in pure RTIL solution and solution containing 10% vol. organic solvent show non-uniform coloring, with the sample charged in solution containing

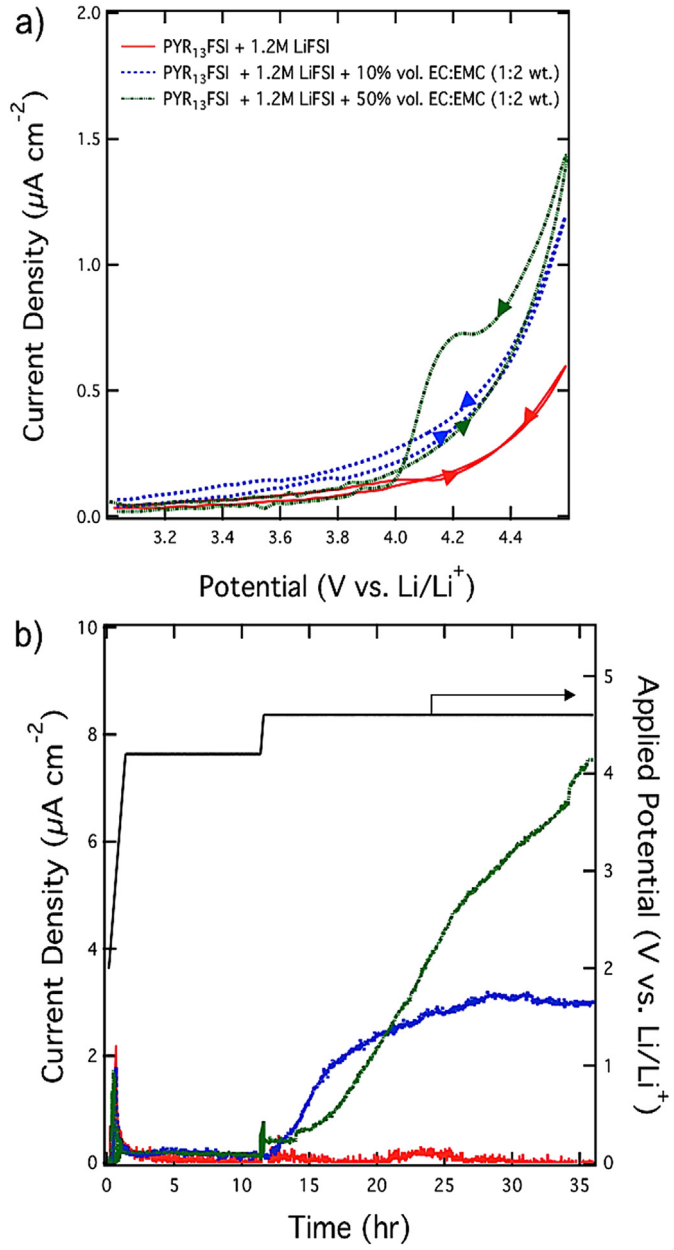

Fig. 2. Cyclic voltammograms (a) showing the first voltage scans and chronoamperograms (b) of aluminum corrosion cells with electrolyte solutions comprised of mixtures of $PYR_{13}FSI$ + 1.2 M LiFSI and various volumetric amounts of EC:EMC (1:2 wt.).

10% vol. organic solvent showing severe shading gradients indicative of the formation of surface pits. The SEM micrographs corroborate the CV and chronoamperometry results, showing more severe corrosion in cells containing LiTFSI salt.

While the observed aluminum oxidation was less severe in cells containing the LiFSI salt, SEM micrographs provided in Fig. 3d–f prove that the oxidative current in $PYR_{13}FSI$ + 1.2 M LiFSI solution containing 50% vol. organic solvent was sufficient to form large pits on the surface of the aluminum metal. Pits on this sample were observed with diameters exceeding 150 μm. The Al charged in pure IL shows uniform coloring while the image of the Al charged in a solution of 10% vol. organic solvent shows a non-uniform distribution of regions of lighter or darker coloring. This spotting is most apparent on the Al sample that was charged in a solution of 50% vol. organic solvent, with corrosion sites evolving into surface pitting. The combination of CV, chronoamperometry, and microscopy data suggests that pitting corrosion results from the oxidative dissolution mechanism characterized in $TFSI^-$ based electrolytes [23]. The suggested oxidative dissolution of aluminum occurs through a mechanism initiated by sulfonyl imide anion attack of the native oxide layer on the surface of the aluminum current collector (Al_2O_3) at high potentials (>4.2 V vs. Li/Li^+). The ions subsequently form Al-imide complexes, e.g. $Al(FSI)_3$, which are solvated by organic carbonates in the electrolyte solution, thereby leaving large pits in the aluminum sheet and introducing metal ions into the electrolyte. Furthermore, this study shows that $PYR_{13}FSI$ + 1.2 M LiFSI based electrolytes containing 10% vol. or less of organic solvent suppress aluminum corrosion to a significant degree, especially when exposed to voltages ≤4.2 V vs. Li/Li^+.

3.2. Organic solvent addition and rate performance of $Li(Ni_{1/3}Mn_{1/3}Co_{1/3})O_2$

Despite finding significant aluminum corrosion in mixtures of $PYR_{13}FSI$ + 1.2 M LiFSI and organic solvent, we demonstrate the ability of organic solvent to greatly increase the electrochemical performance of such electrolytes. It is widely accepted that solution viscosity is the most important factor determining an IL's ionic conductivity. Therefore, ILs containing smaller ions, which lead to lower viscosities, are preferred. The relationship between viscosity and conductivity is defined by the Walden Rule, which states that the product of the limiting molar conductivity, Λ_m^o, and the solvent's viscosity, η, is constant [51]. ILs have been found to obey this relationship [49,51], and the addition of organic solvent to ILs is one strategy for lowering solution viscosity [4,37].

This work supports the claim that adding organic solvent to ILs can increase lithium ion conductivity and mobility by showing that addition of a carbonate-based co-solvent to $PYR_{13}FSI$ + 1.2 M LiFSI leads to significantly increased ionic conductivities. Ionic conductivities for $PYR_{13}FSI$-based solutions are provided in Table 1. The benefits of organic solvent addition to ILs are substantiated by a rate study of $Li(Ni_{1/3}Mn_{1/3}Co_{1/3})O_2$ half-cells in mixtures of $PYR_{13}FSI$ + 1.2 M LiFSI and EC:EMC (1:2 wt.). Rate study results are presented in Fig. 4. Cells were cycled at rates from C/10 to 8C between 3 and 4.2 V vs. Li/Li^+. Half-cells containing 50% vol. organic solvent show significantly increased capacities at all rates tested, maintaining specific discharge capacities above 90 mAh g^{-1} at the rate of 8C. This contrasts the rate performance of cells containing pure IL, which show capacities of approximately 56 mAh g^{-1} at the 8C rate.

Furthermore, $Li(Ni_{1/3}Mn_{1/3}Co_{1/3})O_2$ half-cells show highly stable cycling behavior for at least 25 cycles at the rate of 1C subsequent to the rate test, with cells containing 50% vol. organic solvent and 10% vol. organic solvent maintaining >98% discharge capacity and cells containing pure IL maintaining >99% discharge capacity. Because the specific capacities during rate increase steps (increasing rates in steps from 1C to 8C) are equal to the corresponding specific capacities during decreasing rate steps, it is suggested that the IL based electrolytes do not induce degradation of the $Li(Ni_{1/3}Mn_{1/3}Co_{1/3})O_2$ structure under high current densities.

In order to further investigate the effect of organic solvent addition to ILs on electrochemical performance, lithium ion transference numbers ($t_{+,\,Li}$) were determined for each solution utilized in the rate study. $t_{+,\,Li}$, which is defined as the fraction of the total current passed through the cell by Li^+ ions, has implications for rate performance and cycling stability [50]. While σ_{ionic} describes the electrolyte solution's contribution to ohmic overpotential losses during electrochemical cycling, $t_{+,\,Li}$ describes contributions to

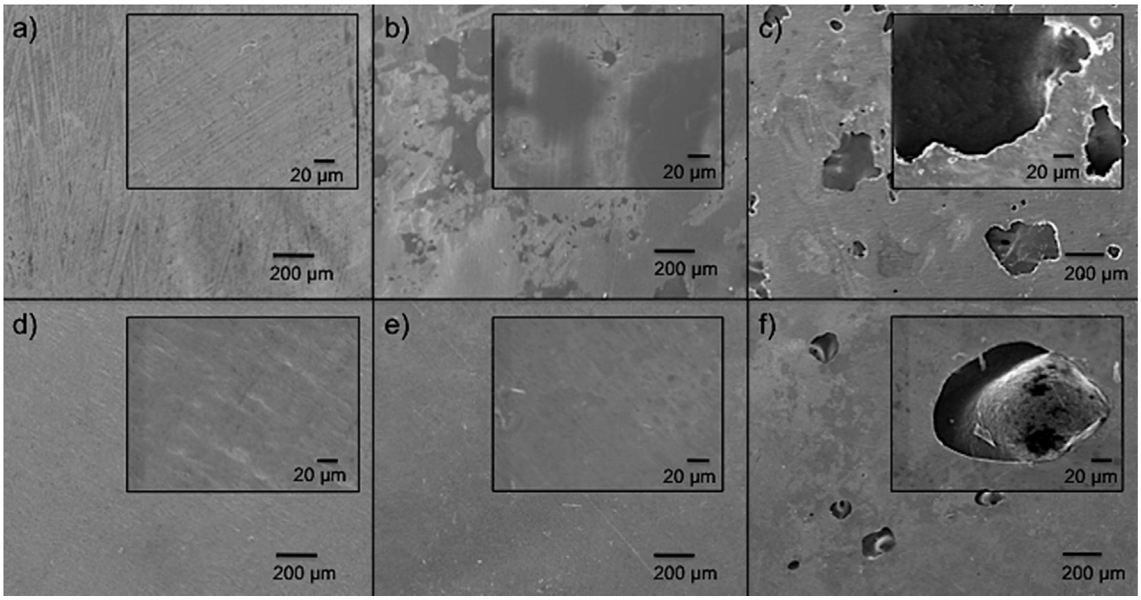

Fig. 3. SEM micrographs taken subsequent to extended charging of Al corrosion cells at 4.6 V vs. Li/Li^+ in electrolyte solutions comprised of pure $PYR_{13}FSI$ + 1.2 M LiTFSI (a), 1.2 M LiTFSI in $PYR_{13}FSI$ + 10% vol. EC:EMC (b), 1.2 M LiTFSI in $PYR_{13}FSI$ + 50% vol. EC:EMC (c), pure $PYR_{13}FSI$ + 1.2 M LiFSI (d), 1.2 M LiFSI in $PYR_{13}FSI$ + 10% vol. EC:EMC (e), and 1.2 M LiFSI in $PYR_{13}FSI$ + 50% vol. EC:EMC (f).

Table 1
Lithium transference numbers, specific ionic conductivities, and aluminum oxidation charge transfer coefficients for electrolyte solutions comprised of mixtures of $PYR_{13}FSI$ + 1.2 M LiFSI and various volumetric amounts of EC:EMC (1:2 wt.). All measurements were conducted at room temperature.

Electrolyte composition	$t_{+,\,Li}$	σ_{ionic} (mS cm^{-1})
PC (1.5 M $LiPF_6$)	0.37125 ± 0.0493	–
$PYR_{13}FSI$ (1.2 M LiFSI)	0.14769 ± 0.0328	3.9735 ± 0.3413
$PYR_{13}FSI$ + 10% vol. EC:EMC (1.2 M LiFSI)	0.19785 ± 0.0405	5.0322 ± 0.1501
$PYR_{13}FSI$ + 50% vol. EC:EMC (1.2 M LiFSI)	0.40968 ± 0.0584	7.8639 ± 1.254

concentration overpotential losses. It follows that a low $t_{+,\,Li}$ limits power output and leads to poor performance at high rates, whereas a high $t_{+,\,Li}$ reduces the effects of concentration polarization while allowing for high power output.

$t_{+,\,Li}$ was determined through the PP method developed by Bruce and Vincent et al., in which the cation transference number is determined by dividing the steady-state cationic current by the initial current passing through the cell just after applying a small polarizing voltage [46,47]. For small polarizations, $t_{+,\,Li}$ is found using Equation (1), where I_{ss} is the steady-state current, I_0 the initial current, ΔV the applied potential (10 mV), and R_{ss} and R_0 the electrode–electrolyte interfacial resistances after and before polarization, respectively [48].

$$t_{+,Li} = \frac{I_{SS}(\Delta V - I_0 R_0)}{I_0(\Delta V - I_{SS} R_{SS})} \quad (1)$$

In order to ensure accuracy of our experiments, the PP method was verified using 1.5 M $LiPF_6$ propylene carbonate (PC) solution and the results were found to agree with literature values [52]. The

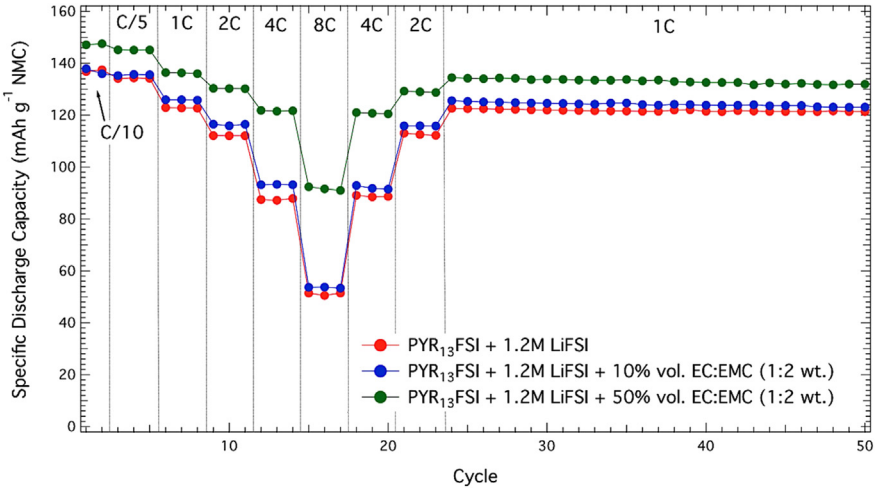

Fig. 4. Rate study of $Li(Ni_{1/3}Mn_{1/3}Co_{1/3})O_2$ half-cells containing electrolyte solutions comprised of mixtures of $PYR_{13}FSI$ + 1.2 M LiFSI and various volumetric amounts of EC:EMC (1:2 wt.). Electrochemical cycling was performed at room temperature between 3 and 4.2 V vs. Li/Li^+.

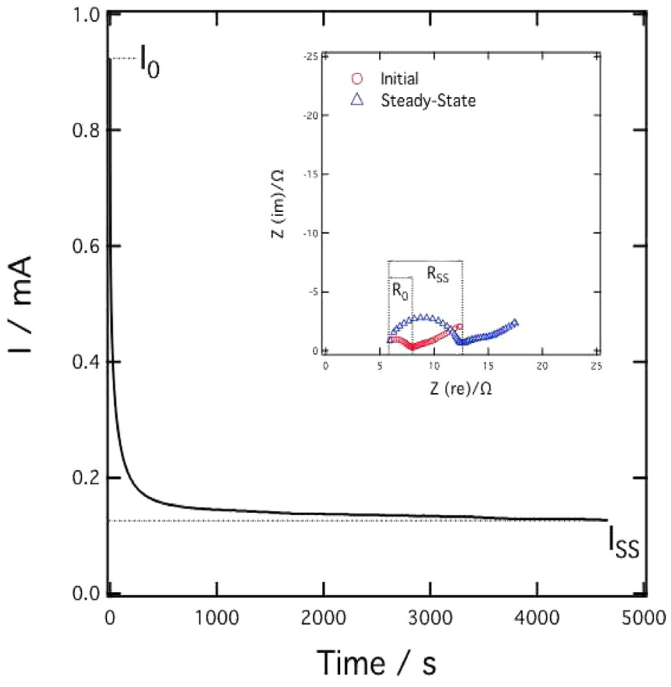

Fig. 5. PP method data for extraction of $t_{+,\,Li}$ for $PYR_{13}FSI$ + 1.2 M LiFSI.

PP method data for the pure ionic liquid sample is shown in Fig. 5 and is representative of PP method data for all samples. $t_{+,\,Li}$ values for the $PYR_{13}FSI$-based solutions are provided in Table 1. The $t_{+,\,Li}$ value determined for the pure IL electrolyte was 0.14769 ± 0.0328, which correlates with literature $t_{+,\,Li}$ values for $PYR_{13}FSI$ based electrolytes [50]. It was found that $t_{+,\,Li}$ of $PYR_{13}FSI$ + 1.2 M LiFSI electrolytes increases significantly with the addition of organic solvent. As organic solvent is added to the IL solutions, the relative concentrations of PYR_{13}^{+} and FSI^{-} decrease while Li^{+} concentration remains fixed at 1.2 M. It is suggested that the effects of two-cation competition decrease as the relative concentration of PYR_{13}^{+} decreases, allowing Li^{+} to carry a larger portion of faradic current during cycling. Consequently, it is expected that the concentration gradients which develop during charge and discharge of electrochemical cells containing 1.2 M LiFSI in $PYR_{13}FSI$ + 50% vol. EC:EMC are significantly less severe than those which develop in the pure IL electrolyte. The higher values of $t_{+,\,Li}$ in IL based electrolytes containing organic solvent contribute to their higher rate performance in our $Li(Ni_{1/3}Mn_{1/3}Co_{1/3})O_2$ half-cells. In addition to providing high-rate cycling stability, the significantly higher $t_{+,\,Li}$ value for the $PYR_{13}FSI$ electrolyte containing 50% vol. organic solvent allows for remarkably less overpotential loss during charge–discharge cycling. Overpotential effects are illustrated by comparing cycling voltage profiles provided in Fig. 6. This phenomenon is particularly evident as the rates are increased, demonstrating the value of high $t_{+,\,Li}$ and its relationship to electrochemical cycling behavior.

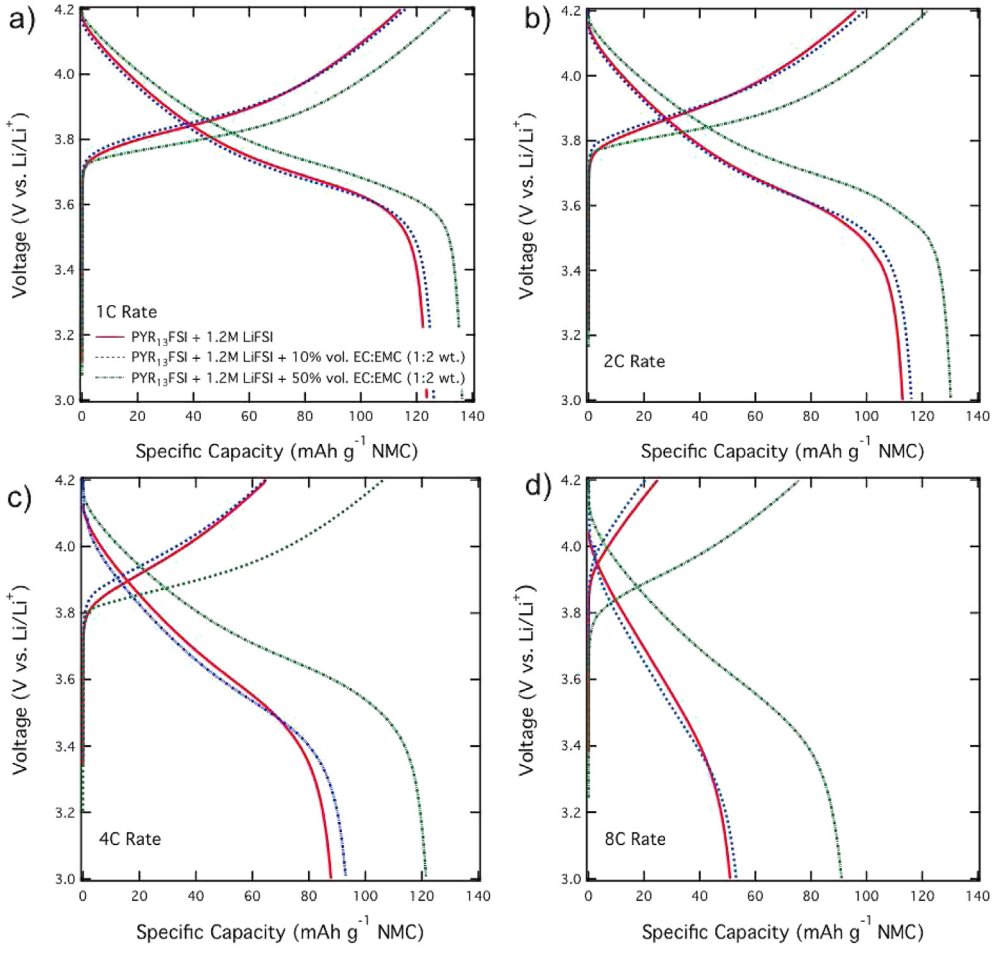

Fig. 6. Charge–discharge voltage profiles of $Li(Ni_{1/3}Mn_{1/3}Co_{1/3})O_2$ half-cells containing electrolyte solutions comprised of mixtures of $PYR_{13}FSI$ + 1.2 M LiFSI and various volumetric amounts of EC:EMC (1:2 wt.) at rates of 1C (a), 2C (b), 4C (c), and 8C (d).

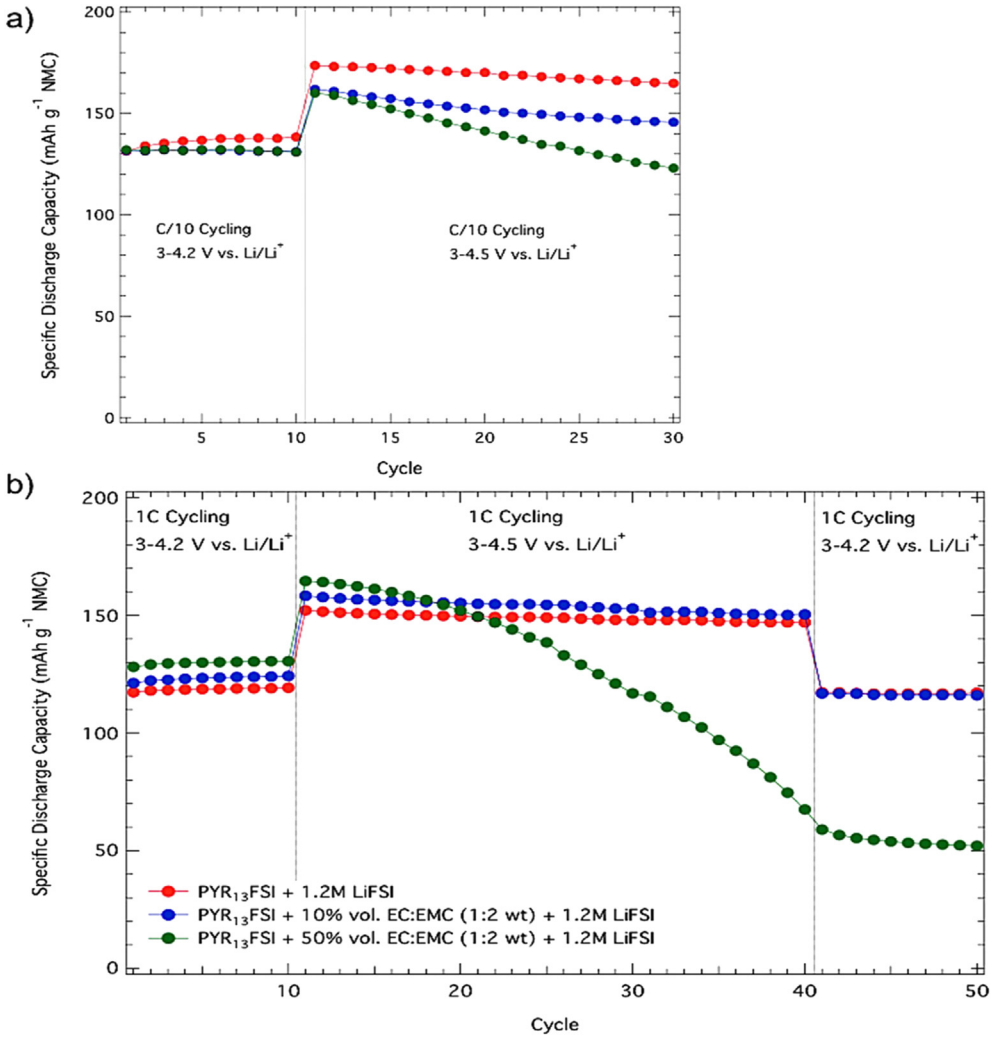

Fig. 7. High voltage potentio-galvanostatic cycling of $Li(Ni_{1/3}Mn_{1/3}Co_{1/3})O_2$ half-cells containing electrolyte solutions comprised of mixtures of $PYR_{13}FSI$ + 1.2 M LiFSI and various volumetric amounts of EC:EMC (1:2 wt.). Charge/discharge rates were held constant at C/10 (a) and 1C (b).

In order to fully realize the advantages in energy and power density of high-voltage cathode materials such as $Li(Ni_{1/3}Mn_{1/3}Co_{1/3})O_2$, electrochemical cells containing such materials should be cycled to voltages higher than 4.2 V vs. Li/Li^+. Fig. 7 provides specific discharge capacities for $Li(Ni_{1/3}Mn_{1/3}Co_{1/3})O_2$ half-cells containing each electrolyte solution under high voltage cycling conditions. $Li(Ni_{1/3}Mn_{1/3}Co_{1/3})O_2$ cells show very poor cycling stability when cycled between 3 and 4.5 V vs. Li/Li^+. While half-cells containing pure IL maintain >95% capacity after 20 cycles at a rate of C/10 during cycling between 3 and 4.5 V vs. Li/Li^+, cells containing 10% vol. organic solvent and 50% vol. organic solvent maintain only >85% capacity and >75% capacity, respectively, under the same cycling conditions (Fig. 7a). The poor cycling stability is exacerbated at higher rates and is shown to be irreversible, as the capacity lost during high voltage cycling is not recovered when the cycling voltage range is lowered to 3–4.2 V vs. Li/Li^+ (Fig. 7). The poor cycling stability is attributed to the introduction of aluminum into the electrolyte following the oxidative dissolution process, most likely leading to increased resistance through the bulk of the cell and possibly leading to performance-limiting interactions with the layered cathode material.

While the addition of organic solvent to $PYR_{13}FSI$ + 1.2 M LiFSI is shown to lead to a parasitic oxidation reaction with the aluminum current collector conventionally used in lithium-ion batteries, the enhancements in conductivity, lithium transference number, and rate performance are significant. It is therefore of great interest to suppress the aluminum oxidation process in order to enable high performance ionic liquid based electrolytes for application in lithium-ion batteries.

4. Conclusions

In this paper we demonstrated that $PYR_{13}FSI$ + 1.2 M LiFSI shows higher compatibility with aluminum current collectors than $PYR_{13}FSI$ + 1.2 M LiTFSI electrolytes. The oxidation of aluminum in such IL solutions increases with addition of organic solvent, and the oxidative dissolution mechanism was characterized in corrosion cells containing LiFSI salt in $PYR_{13}FSI$. Furthermore, we demonstrated that the addition of organic solvent to the $PYR_{13}FSI$ + 1.2 M LiFSI electrolyte leads to higher ionic conductivities and higher lithium transference numbers, and these enhanced electrochemical properties allow for significantly increased rate performance in $Li(Ni_{1/3}Mn_{1/3}Co_{1/3})O_2$ half-cells when cycled at room temperature between 3 and 4.2 V vs. Li/Li^+. The use of organic solvents in combination with ILs was substantiated as a convenient and

effective strategy for the realization of high performance, non-flammable electrolyte solutions for lithium-ion batteries.

Acknowledgments

The authors would like to thank Mr. Steve Pred (Pred Materials International, Inc.) for supply of Al-clad 2032 coin-type cells. Funding for this work comes from Boulder Ionics Corporation through the Membrane Science, Engineering and Technology (MAST) Center at CU-Boulder, an NSF Industry-University Cooperative Research Center. This material is based upon work supported by the National Science Foundation under Grant No. IIP-1152040. Any opinions, findings, and conclusions or recommendations expressed in this material are those of the author(s) and do not necessarily reflect the views of the National Science Foundation.

References

[1] M. Park, X. Zhang, M. Chung, G.B. Less, A.M. Sastry, J. Power Sources 195 (2010) 7904.
[2] K. Xu, Chem. Rev. 104 (2004) 4303.
[3] A. Balducci, S.S. Jeong, G.T. Kim, S. Passerini, M. Winter, M. Schmuck, A.B. Appetecchi, R. Marcilla, D. Mecerreyes, V. Barsukov, V. Khomenko, I. Cantero, I. De Meatza, M. Holzapfel, N. Tran, J. Power Sources 196 (2011) 9719.
[4] D. Moosbauer, S. Zugmann, M. Amereller, H.J. Gores, J. Chem. Eng. Data 55 (2010) 1794.
[5] B. Scrosati, J. Garche, J. Power Sources 195 (2010) 2419.
[6] A. Fernicola, B. Scrosati, H. Ohno, Ionics 12 (2006) 95.
[7] M. Armand, F. Endres, D.R. MacFarlane, H. Ohno, B. Scrosati, Nat. Mater. 8 (2009) 621.
[8] S. Seki, Y. Kobayashi, H. Miyashiro, Y. Ohno, A. Usami, Y. Mita, N. Kihira, M. Watanabe, N. Terada, J. Phys. Chem. B 110 (2006) 10228.
[9] H.B. Han, S.S. Zhou, D.J. Zhang, S.W. Feng, L.F. Li, K. Liu, W.F. Feng, J. Nie, H. Li, X.J. Huang, M. Armand, Z.B. Zhou, J. Power Sources 196 (2011) 3623.
[10] A.P. Lewandowski, A.F. Hollenkamp, S.W. Donne, A.S. Best, J. Power Sources 195 (2010) 2029.
[11] J. Reiter, M. Nádherná, R. Dominko, J. Power Sources 205 (2012) 402.
[12] H. Sakaebe, H. Matsumoto, Electrochem. Commun. 5 (2003) 594–598.
[13] B. Garcia, S. Lavallér, G. Perron, Ch. Michot, M. Armand, Electrochim. Acta 49 (2004) 4583–4588.
[14] M. Holzapfel, C. Jost, A. Prodi-Schwab, F. Krumeich, A. Würsig, H. Buqa, P. Novák, Carbon 43 (2005) 1488–1498.
[15] H. Sakaebe, H. Matsumoto, K. Tatsumi, J. Power Sources 146 (2005) 693–697.
[16] H. Matsumoto, H. Sakaebe, K. Tatsumi, M. Kikuta, E. Ishiko, M. Kono, J. Power Sources 160 (2006) 1308–1313.
[17] M. Egashira, M. Tanaka-Nakagawa, I. Watanabe, S. Okada, J.I. Yamaki, J. Power Sources 160 (2006) 1387–1390.
[18] S. Seki, Y. Ohno, Y. Kobayashi, H. Miyashiro, A. Usami, Y. Mita, H. Tokuda, M. Watanabe, K. Hayamizu, S. Tsuzuki, J. Electrochem. Soc. 154 (2007) A173–A177.
[19] N.S. Choi, Y. Lee, S.S. Kim, S.C. Shin, Y.M. Kang, J. Power Sources 195 (2010) 2368–2371.
[20] S.F. Lux, M. Schnuck, G.B. Appetecchi, S. Passerini, M. Winter, A. Balducci, J. Power Sources 192 (2009) 606–611.
[21] M. Nadherna, J. Reiter, J. Moskon, R. Dominko, J. Power Sources 196 (2011) 7700–7706.
[22] G.B. Appetecchi, M. Montanino, A. Balducci, S.F. Lux, M. Winterb, S. Passerini, J. Power Sources 192 (2009) 599.
[23] R.S. Kühnel, M. Lübke, M. Winter, S. Passerini, A. Balducci, J. Power Sources 214 (2012) 178.
[24] A. Fernicola, F. Croce, B. Scrosati, T. Watanabe, H. Ohno, J. Power Sources 174 (2007) 342.
[25] M. Ishikawa, T. Sugimoto, M. Kikuta, E. Ishiko, M. Kono, J. Power Sources 162 (2006) 658.
[26] R.S. Kühnel, N. Böckenfeld, S. Passerini, M. Winter, A. Balducci, Electrochim. Acta 56 (2011) 4092.
[27] A. Guerfi, S. Duchesne, Y. Kobayashi, A. Vijh, K. Zaghib, J. Power Sources 175 (2008) 866.
[28] T. Sugimoto, Y. Atsumi, M. Kikuta, E. Ishiko, M. Kono, M. Ishikawa, J. Power Sources 189 (2009) 802–805.
[29] A.S. Best, A.I. Bhatt, A.F. Hollenkamp, J. Electrochem. Soc. 157 (2010) A903.
[30] K. Zaghib, P. Charest, A. Guerfi, J. Shim, M. Perrier, K. Striebel, J. Power Sources 134 (2004) 124.
[31] K. Kubota, T. Nohira, T. Goto, R. Hagiwara, Electrochem. Commun. 10 (2008) 1886.
[32] A.I. Bhatt, A.S. Best, J. Huang, A.F. Hollenkamp, J. Electrochem. Soc. 157 (2010) A66.
[33] Y. Wang, K. Zaghib, A. Guerfi, F.F.C. Bazito, R.M. Torresi, J.R. Dahn, Electrochim. Acta 52 (2007) 6346.
[34] E. Paillard, Q. Zhou, W.A. Henderson, G.B. Appetecchi, M. Montanino, S. Passerini, J. Electrochem. Soc. 156 (2009) A891.
[35] A. Abouimrane, J. Ding, I.J. Davidson, J. Power Sources 189 (2009) 693.
[36] Q. Zhou, W. Henderson, G.B. Appetecchi, M. Montanino, S. Passerini, J. Phys. Chem. B 112 (2008) 13580.
[37] A. Guerfi, M. Dontigny, P. Charest, M. Petitclerc, M. Lagacé, A. Vigh, K. Zaghib, J. Power Sources 195 (2010) 845.
[38] H.S. Lee, X.Q. Yang, X. Sun, J. McBreen, J. Power Sources 97–98 (2001) 566.
[39] M. Holzpfel, C. Jost, P. Novak, Chem. Commun. 4 (2004) 2098.
[40] T. Sato, M. Maruo, S. Marukane, K. Takagi, J. Power Sources 138 (2004) 253.
[41] Y. An, P. Zuo, C. Du, Y. Ma, X. Cheng, J. Lin, G. Yin, RSC Adv. 2 (2012) 4097.
[42] Z. Chen, W.Q. Lu, J. Liu, K. Amine, Electrochim. Acta 51 (2006) 3322.
[43] W.Q. Lu, Z.H. Chen, H. Joachin, J. Power Sources 163 (2007) 1074.
[44] E. Cho, J. Mun, O.B. Chae, O.M. Kwon, H.T. Kim, J.H. Ryu, Y.G. Kim, S.M. Oh, Electrochem. Commun. 22 (2012) 1.
[45] B. Garcia, M. Armand, J. Power Sources 132 (2004) 206.
[46] P.G. Bruce, C.A. Vincent, J. Electroanal. Chem. 225 (1987) 1.
[47] P.G. Bruce, J. Evans, C.A. Vincent, Solid State Ionics 28-30 (1988) 918.
[48] S. Zugmann, M. Fleischmann, M. Amereller, R.M. Gschwind, H.D. Wiemhöfer, H.J. Gores, Electrochim. Acta 56 (2011) 3926.
[49] K. Hayamizu, Y. Aihara, H. Nakagawa, T. Nukuda, W.S. Price, J. Phys. Chem. B 108 (2004) 19527.
[50] H. Yoon, P.C. Howlett, A.S. Best, M. Forsyth, D.R. MacFarlane, J. Electrochem. Soc. 160 (2013) A12629.
[51] C. Schreiner, S. Zugmann, R. Hartl, H.J. Gores, J. Chem. Eng. Data 55 (2010) 1784.
[52] T. Froemling, M. Kunze, M. Schoenhoff, J. Sundermeyer, B. Roling, J. Phys. Chem. B 112 (2008) 12985.